COMPUTATIONAL MECHANICS 2021
36th conference with international participation
Srní
November 8 - 10, 2021

A high order discontinuous Galerkin method for fluid-structure interaction

O. Winter[a,b], P. Sváček[a,b]

[a] Dept. of Instrumentation and Control Engineering, Faculty of Mechanical Engineering, Center of Advanced Aerospace Technology, Czech Technical University in Prague, Technicka Street 4, 166 07, Prague 6, Czech Republic

[b] Dept. of Technical Mathematics, Faculty of Mechanical Engineering, Czech Technical University in Prague, Charles Square 13, 120 00, Prague 2, Czech Republic

1. Introduction

Many important scientific and engineering problems require analysis of fluid-structure interaction (FSI). For example, aeroelastic flutter can produce large and potentially destructive vibrations in aircraft [7], turbines [1], and other structures [3] or biological applications such as study of fluid flow inside human vocal tract [5]. The presented study deals with a high order discontinuous Galerkin method for fluid-structure interaction.

2. Mathematical model

The model consists of the Navier-Stokes equations governing the motion of a compressible fluid flow coupled to a rigid body dynamics, i.e., a movement of a structure, described by a second order ordinary differential equation. Arbitrary Lagrangian Eulerian (ALE) method is used to treat the deformable domain. The viscous gas dynamics in computational domain $\Omega_t \subset \mathbb{R}^2$ for any $t \in (0,T), T > 0$ is described by the Navier-Stokes equations, see e.g. [2]. The Navier-Stokes equations written in the conservative form reads

$$\begin{aligned} \frac{\partial}{\partial t}(\varrho) + \sum_{i=1}^{2} \frac{\partial}{\partial x_i}(\varrho v_i) &= 0, \\ \frac{\partial}{\partial t}(\varrho v_i) + \sum_{j=1}^{2} \frac{\partial}{\partial x_j}(\varrho v_i v_j + p\delta_{ij}) &= \sum_{j=1}^{2} \frac{\partial}{\partial x_j}(\tau_{ij}), \quad \text{for } i = 1,2, \\ \frac{\partial}{\partial t}(\varrho E) + \sum_{j=1}^{2} \frac{\partial}{\partial x_j}(\varrho v_j E + v_j p) &= \sum_{j=1}^{2} \frac{\partial}{\partial x_j}(-q_j + v_i \tau_{ij}), \end{aligned} \tag{1}$$

where ϱ is the fluid density, p is the pressure, v_1, v_2 are the velocity components of the velocity vector $\boldsymbol{v}$, and E is the total energy. The components of the viscous stress tensor $\boldsymbol{\tau}$ and the heat flux $\boldsymbol{q}$ are given by

$$\tau_{ij} = \mu \left(\frac{\partial v_i}{\partial x_j} + \frac{\partial v_j}{\partial x_i} - \sum_{k=1}^{2} \frac{2}{3} \frac{\partial v_k}{\partial x_k} \delta_{ij} \right) \tag{2}$$

and

$$q_i = \frac{\mu}{\mathrm{Pr}} \frac{\partial}{\partial x_i} \left(E + \frac{p}{\varrho} - \sum_{j=1}^{2} \frac{1}{2} v_j v_j \right), \tag{3}$$

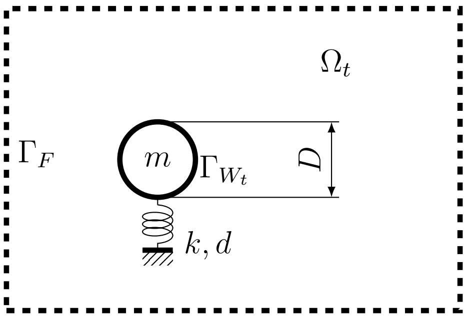

Fig. 1. Sketch of the computation domain Ω_t

where μ is dynamic viscosity and Pr, assumed to be constant $\mathrm{Pr} = 0.72$, is the Prandtl number. For an ideal gas, the pressure p has the form

$$p = (\gamma - 1)\varrho \left(E - \frac{1}{2}\sum_{i=1}^{2} v_i v_i \right), \tag{4}$$

where γ is the adiabatic gas constant, γ is set to 1.4 in presented study. Imposed boundary conditions are either free-stream at the far field, or adiabatic no-slip conditions at the boundaries of the structure, i.e., $\boldsymbol{v}|_{\Gamma_{W_t}}$ is equal to the velocity of the structure. System (1) is supplemented with suitable initial conditions.

The motion of the structure in the one-direction is modeled by the second-order differential linear equation, i.e.,

$$m\ddot{h} + d\dot{h} + kh = L, \tag{5}$$

where m is the oscillating mass of the system, d and k denote the mechanical damping and stiffness of the oscillator unit, respectively, h is the displacement of the oscillator and L is the force exerted by the fluid on the structure in the transverse direction, see Fig 1. Fluid flow model (1) is coupled with the rigid body model (5) via L in the following manner, i.e.,

$$L = -l \int_{\Gamma_{W_t}} \sum_{j=1}^{2} (\tau_{2j} - p\delta_{2j}) n_j \, dS, \tag{6}$$

where l is the depth of the structure, $\boldsymbol{n} = (n_1, n_2)$ is the unit outer normal to $\partial\Omega_t$ on Γ_{W_t} (pointing into the structure). System (5) is supplemented with initial suitable initial conditions.

3. Numerical approximation

The fluid flow model is discretized using a high-order discontinuous Galerkin formulation with triangular grid elements and nodal basis functions and the domain movement is taken into account with aid of arbitrary Lagrangian-Eulerian method, see e.g. [7]. Following standard procedure for DG discretization of second-derivatives, first the auxiliary gradient variable $\boldsymbol{g}$ is introduced, and then governing equations are rewritten as the system of first order equations, i.e.,

$$\frac{\partial}{\partial t}(\boldsymbol{u}) + \nabla \cdot \boldsymbol{F}^i(\boldsymbol{u}) - \nabla \cdot \boldsymbol{F}^v(\boldsymbol{u}, \boldsymbol{g}) = \boldsymbol{0}, \tag{7}$$

$$\nabla \boldsymbol{u} = \boldsymbol{g}, \tag{8}$$

where $\boldsymbol{u} = [\varrho, \varrho v_1, \varrho v_2, \varrho E]^T$ is the solution vector, $\boldsymbol{F}^i$ is inviscid flux given as

$$\boldsymbol{F}^i(\boldsymbol{u}) = \begin{bmatrix} \varrho v_1 & \varrho v_2 \\ \varrho v_1 v_1 & \varrho v_2 v_1 \\ \varrho v_1 v_2 & \varrho v_2 v_2 \\ (\varrho E + p) v_1 & (\varrho E + p) v_2 \end{bmatrix} \tag{9}$$

and $\boldsymbol{F}^v$ is viscous flux given as

$$\boldsymbol{F}^v(\boldsymbol{u}, \boldsymbol{g}) = \begin{bmatrix} 0 & 0 \\ \tau_{11}(\boldsymbol{g}) & +\tau_{12}(\boldsymbol{g}) \\ \tau_{21}(\boldsymbol{g}) & +\tau_{22}(\boldsymbol{g}) \\ -q_1(\boldsymbol{u}) + v_1\tau_{11}(\boldsymbol{g}) + v_2\tau_{21}(\boldsymbol{g}) & -q_2(\boldsymbol{u}) + v_1\tau_{12}(\boldsymbol{g}) + v_2\tau_{22}(\boldsymbol{g}) \end{bmatrix}. \tag{10}$$

The inviscid fluxes are computed using Roe's method [6], and the numerical fluxes for the viscous terms are chosen according to the compact discontinuous Galerkin (CDG) method [4]. The computational domain Ω is discretized by the computational mesh with elements $\mathcal{T}_h = \{K\}$. The solution $(\boldsymbol{u}, \boldsymbol{g})$ is sought in $[V_h^p]^4$ and $[V_h^p]^{4\times 2}$, respectively, where $V_h^p = \{v \in L^2(\Omega), v|_K \in P^p(K), \forall K \in \mathcal{T}_h\}$ with P^p being the space of polynomial functions of degree at most $p \geq 1$ on K. The semi-discrete DG formulation is expressed as: find $\boldsymbol{u}_h \in [V_h^p]^4$ and $\boldsymbol{g}_h \in [V_p^h]^{4\times 2}$ such that for all $K \in \mathcal{T}_h$

$$\begin{aligned} \int_K \frac{\partial \boldsymbol{u}_h}{\partial t} \cdot \boldsymbol{\varphi} + \int_K (\boldsymbol{F}^i(\boldsymbol{u}_h) - \boldsymbol{F}^v(\boldsymbol{u}_h, \boldsymbol{g}_h)) : \nabla\boldsymbol{\varphi} - \\ - \int_{\partial K} (\boldsymbol{F}^i(\boldsymbol{u}_h) - \boldsymbol{F}^v(\boldsymbol{u}_h, \boldsymbol{g}_h)) \cdot \boldsymbol{\varphi} = \boldsymbol{0}, \quad \forall \boldsymbol{v} \in [P^p(K)]^4, \end{aligned} \tag{11}$$

$$\int_K \boldsymbol{g}_h : \boldsymbol{\psi} + \int_K \boldsymbol{u}_h \cdot (\nabla \cdot \boldsymbol{\psi}) - \int_{\partial K} (\boldsymbol{u}_h \otimes \boldsymbol{n}) : \boldsymbol{\psi} = \boldsymbol{0}, \quad \forall \boldsymbol{\psi} \in [P^p(K)]^{4\times 2}. \tag{12}$$

Fluxes in Eqs. (11) and (12) are modified according to the ALE method, see e.g. [7]. All integrals in Eqs. (11) and (12) are integrated using high-order Gaussian quadrature rules. Time integration is done with aid of a high-order Runge-Kutta (RK) method.

4. Numerical results

To validate the high-order scheme, we considered a test problem consisting of flow-induced vibration of a circular cylinder, where the cylinder is allowed to move in vertical direction, see Fig. 1. The far field fluid has velocity $\boldsymbol{v} = (1, 0)\,\mathrm{m/s}$, density $\varrho = 1\,\mathrm{kg/m^3}$, Mach is equal to 0.2, and a Reynolds number with respect to diameter D is equal to 100. The constants chosen for this problem were $D = 1\,\mathrm{m}$, $m = 1\,\mathrm{kg}$, $k = 0.64\,\mathrm{N/m}$, $d = 10^{-3}k\,\mathrm{Ns/m}$, and $l = 1\,\mathrm{m}$. Fig. 2 shows position h of the cylinder during the computation. Numerical solutions for two cases of our discontinuous Galerkin scheme (RK2-DG1 – second order RK method, first order of polynomials, RK4-DG3 – fourth order RK method, third order of polynomials) are compared to finite volume approximation on very fine grid these solutions indicate very good converge of our scheme.

Acknowledgements

This work was supported by the Grant Agency of the Czech Technical University in Prague (SGS19/154/OHK2/3T/12). Authors acknowledge support from the ESIF, EU Operational Programme Research, Development and Education, and from the Center of Advanced Aerospace Technology (CZ.02.1.01/0.0/0.0/16_019/0000826), Faculty of Mechanical Engineering, Czech Technical University in Prague.

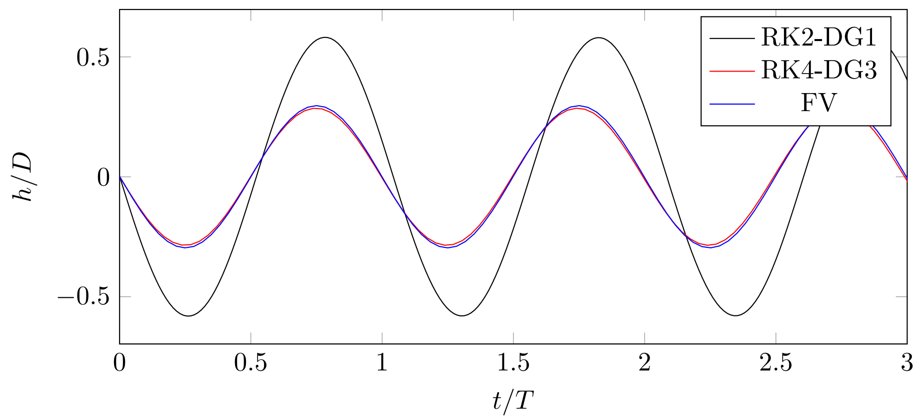

Fig. 2. Position of the cylinder h during selected time period

References

[1] Badur, J., Bryk, M., Accelerated start-up of the steam turbine by means of controlled cooling steam injection, Journal of Energy 173 (2019) 1242-1255.

[2] Blažek, J., Computational fluid dynamics: Principles and applications, Elsevier, 3rd edition, 2015.

[3] Hoseini, S. S., Najafi, G., Ghobadian, B., Akbarzadeh, A. H., Impeller shape-optimization of stirred-tank reactor: CFD and fluid structure interaction analyses, Chemical Engineering Journal 413 (2021) No. 127497.

[4] Peraire, J., Persson, P. O., The compact discontinuous Galerkin (CDG) method for elliptic problems, SIAM Journal on Scientific Computing 30 (4) (2008) 1806-1824.

[5] Sváček, P., Horáček, J., FE numerical simulation of incompressible airflow in the glottal channel periodically closed by self-sustained vocal folds vibration, Journal of Computational and Applied Mathematics 393 (2021) No. 113529.

[6] Toro, E. F., Riemann solvers and numerical methods for fluid dynamics, Springer, 3rd edition, 2009.

[7] Winter, O., Sváček, P., On numerical simulation of flexibly supported airfoil in interaction with incompressible fluid flow using laminar-turbulence transition model, Computers & Mathematics with Applications 83 (2021) 57-73.